NUCL SCI TECH (2019) 30:6
https://doi.org/10.1007/s41365-018-0527-5

Element analysis method of concealed explosive based on TNA

Meng Huang[1] · Jian-Yu Zhu[2] · Jun Wu[2] · Rui Li[3]

Received: 24 January 2018 / Revised: 4 May 2018 / Accepted: 3 June 2018 / Published online: 2 January 2019

Abstract The detection technology of concealed bulk explosives is related to social security and national defense construction and has important research significance. In this paper, an element analysis method of concealed explosives based on thermal neutron analysis is proposed. This method could provide better reconstruction precision for hydrogen, carbon, and nitrogen ratios, making it possible to discriminate explosives from other compounds with the same elements but different proportions, as well as to identify the types of concealed bulk explosives. In this paper, the basic principles and mathematical model of this method are first introduced, and the calculation formula of the element number ratio (the ratio between the nucleus numbers of two different elements) of the concealed explosive is deduced. Second, a numerical simulation platform of this method was established based on the Monte Carlo JMCT code. By calibrating the absorption efficiencies of the explosive device to γ rays, the element number ratios of a concealed explosive model under the irradiation of thermal neutrons were reconstructed from the neutron capture prompt γ-ray spectrum. The reconstruction values were in good agreement with the actual values, which shows that this method has a high reconstruction precision of the element number ratio for concealed explosives. Lastly, it was demonstrated using the simulation study that this method can discriminate explosives, drugs, and common materials, with the capability of determining the existence of concealed bulk explosives and identifying explosive types.

Keywords Concealed bulk explosive · Explosive type identification · TNA · Element number ratio

1 Introduction

Concealed bulk explosives refer to the bulk explosives in the shielding environment that generally include explosives smuggled in containers, hidden in luggage, and in weapons. The detection technology of concealed bulk explosives is related to social security and national defense construction and has important research significance. At present, the detection techniques of concealed bulk explosives mainly include X/γ-ray imaging [1], the nuclear quadrupole resonance technique [2, 3], the terahertz technique [4], and neutron analysis techniques [5–11]. Neutron analysis techniques are used to detect and discriminate various materials based on the interactions between neutrons and materials. Compared to other explosive detection techniques, neutron analysis techniques have advantages of strong penetration and accurate recognition and are more suitable for detecting concealed bulk explosives.

As one of the neutron analysis techniques, thermal neutron analysis (TNA) can be used to detect the concealed bulk explosives by irradiating the inspected materials with thermal neutrons and detecting the emitted characteristic γ-rays of nuclides [5, 10–18]. The theory of TNA was first

✉ Jian-Yu Zhu
zhujyu@126.com

[1] Institute of Applied Physics and Computational Mathematics, Beijing 100094, China

[2] Center for Strategic Studies, China Academy of Engineering Physics, Beijing 100088, China

[3] Software Center for High Performance Numerical Simulation, China Academy of Engineering Physics, Beijing 100088, China

proposed in the 1980s [5], and many subsequent studies have been carried out. Nowadays, TNA is successfully applied in the detection and determination of hidden explosives in luggage and buried landmines, and some commercial detection devices have been developed [11–14].

Current research on the concealed bulk explosive detection based on TNA shows that the existence determination and type identification of explosives are difficult issues. The existence determination of explosives refers to the discrimination of explosives from other materials in the inspection. The identification of explosive types can improve the determination accuracy of whether a concealed explosive exists and decrease the error rate. However, due to the absorption of the explosive and shield of the characteristic γ-rays of the explosive nuclides, the direct reconstruction of the element number ratios (namely the ratio between the nucleus numbers of two different elements) of the explosive based on the detector counts of the characteristic γ-rays significantly deviates from the actual values and cannot be used to discriminate the explosive from the common materials. As a result, two methods were put forward to try to solve this issue. The first is to calculate the absorption efficiencies of the explosive and shield of the γ-rays based on a numerical simulation and apply the calculated absorption efficiencies in the data analysis to the explosive inspection [15]. This method requires prior knowledge of the components and shape of the explosives and shields, and its reconstruction accuracy of the element number ratios of the explosives is not very reliable. The second method is based on the neural networks learning and template comparison of neutron capture prompt γ-ray spectra [11, 16–18]. This method can be used to discriminate explosives from other materials, but it requires large amounts of sample data and has difficulties in identifying the types of explosives accurately.

In this paper, an element analysis method of concealed explosives based on TNA is proposed. This method has the ability to accurately analyze the element number ratios of explosives by calibrating the absorption efficiencies of the explosive and shield of the γ-rays, with potential applications for the determination of the existence of explosives and identification of explosive types. This paper is organized as follows: Sect. 1 contains the introduction; Sect. 2 presents the basic principles of the element analysis method of concealed explosives based on TNA and establishes the mathematical model of this method; Sect. 3 presents the numerical simulation study of this method; Sect. 4 contains an analysis of the simulation results and discusses the feasibility of this method; and Sect. 5 provides the conclusion.

2 Basic principles

TNA is a neutron analysis technique with the following principle: the inspected material is irradiated by thermal neutron beams, and the (n,γ) reactions between the thermal neutrons and material nuclides produce characteristic γ-rays; by detecting and analyzing the characteristic γ-rays emitted from the material, the detection and identification of the inspected material can be realized.

When TNA is used to detect concealed explosives, the incident thermal neutrons have (n,γ) reactions with the ^{1}H, ^{12}C, ^{14}N, and ^{16}O in the explosives, and the characteristic γ-rays of ^{1}H, ^{12}C, ^{14}N, and ^{16}O are produced, as shown in Table 1. By analyzing the relationship between the number of characteristic γ-rays emitted from the explosive device (including the explosive and shield) and number of explosive nuclei, the element number ratio of the concealed explosive, such as the hydrogen–nitrogen ([H]/[N]), carbon–nitrogen ([C]/[N]), and oxygen–nitrogen ([O]/[N]) ratios, can be deduced.

Assuming that A is a nuclide of the concealed explosive, the characteristic γ-ray of the A(n,γ) reaction would be emitted from the explosive device with a certain probability after being produced. For the nuclide A, the number of characteristic γ-rays emitted from the explosive device with energy E_γ per unit time $[K_A(E_\gamma)]$ can be expressed as:

$$K_A(E_\gamma) = \int_V n_A(\vec{r}) \cdot f_A(E_\gamma) \cdot P(\vec{r}, E_\gamma) \cdot \mathrm{d}V, \quad (1)$$

where $P(\vec{r}, E_\gamma)$ is the average probability that the characteristic γ-rays with energy E_γ that are produced at position $\vec{r}$ are emitted from the explosive device; and $f_A(E_\gamma)$ is the branching ratio of the characteristic γ-ray with energy E_γ. $n_A(\vec{r})$ is the spatial density of the (n,γ) reactions between the nuclide A and neutrons per unit time at position $\vec{r}$ given by:

Table 1 Characteristic γ-rays of (n, γ) reactions of ^{1}H, ^{12}C, ^{14}N, and ^{16}O

Nuclide	Energy of γ-ray (MeV)	Branch ratio (%)
^{1}H	2.22	100
^{12}C	4.95	68
^{14}N	1.88	18.78
	3.68	14.53
	4.51	16.72
	5.27	29.88
	6.32	18.24
	10.83	14.33
^{16}O	1.09	85.4

$$n_{\mathrm{A}}(\vec{r}) = \int N_{\mathrm{A}} \cdot \sigma_{\mathrm{A}}(E_{\mathrm{n}}) \cdot \phi\left(\vec{r}, E_{\mathrm{n}}\right) \cdot \mathrm{d}E_{\mathrm{n}}, \tag{2}$$

where N_{A} is the nucleus density of the nuclide A; E_{n} is the neutron energy; $\sigma_{\mathrm{A}}(E_{\mathrm{n}})$ is the microscopic cross section of the (n,γ) reaction between the neutron with energy E_{n} and nuclide A; and $\phi(\vec{r}, E_{\mathrm{n}})$ is the neutron flux density at position $\vec{r}$.

In the calculation of $n_{\mathrm{A}}(\vec{r})$ using Eq. (2), it was found that as the microscopic cross sections of the (n,γ) reactions of ^{1}H, ^{12}C, ^{14}N, and ^{16}O are in the pure 1/v regime (v is the neutron velocity) in the energy range of 0–1 eV, the values of $\frac{\sigma_{^{1}\mathrm{H}}(E_{\mathrm{n}})}{\sigma_{^{14}\mathrm{N}}(E_{\mathrm{n}})}$, $\frac{\sigma_{^{12}\mathrm{C}}(E_{\mathrm{n}})}{\sigma_{^{14}\mathrm{N}}(E_{\mathrm{n}})}$, and $\frac{\sigma_{^{16}\mathrm{O}}(E_{\mathrm{n}})}{\sigma_{^{14}\mathrm{N}}(E_{\mathrm{n}})}$ are approximately constant for the neutrons with energies below 1 eV. According to the ENDF/B-VI database [19], the values are ~ 4.43, 4.53×10^{-2}, and 2.54×10^{-3} for $\left[\frac{\sigma_{^{1}\mathrm{H}}(E_{\mathrm{n}})}{\sigma_{^{14}\mathrm{N}}(E_{\mathrm{n}})}\right]_{\mathrm{T}}$, $\left[\frac{\sigma_{^{12}\mathrm{C}}(E_{\mathrm{n}})}{\sigma_{^{14}\mathrm{N}}(E_{\mathrm{n}})}\right]_{\mathrm{T}}$, and $\left[\frac{\sigma_{^{16}\mathrm{O}}(E_{\mathrm{n}})}{\sigma_{^{14}\mathrm{N}}(E_{\mathrm{n}})}\right]_{\mathrm{T}}$, respectively, and their relative standard deviations are much less than 1% (see Fig. 1). Since the energies of almost all of the neutrons inside the explosive under irradiation of thermal neutrons are less than 1 eV, the equations for $n_{\mathrm{A}}(\vec{r})$ of ^{1}H, ^{12}C, and ^{16}O can be simplified. For example, the equation for $n_{\mathrm{A}}(\vec{r})$ of ^{1}H can be rewritten as:

$$n_{^{1}\mathrm{H}}(\vec{r}) \approx \frac{N_{^{1}\mathrm{H}}}{N_{^{14}\mathrm{N}}} \cdot \left[\frac{\sigma_{^{1}\mathrm{H}}(E_{\mathrm{n}})}{\sigma_{^{14}\mathrm{N}}(E_{\mathrm{n}})}\right]_{\mathrm{T}} \cdot n_{^{14}\mathrm{N}}(\vec{r}). \tag{3}$$

Furthermore, the equation for the number ratio between the characteristic γ-rays of ^{1}H and ^{14}N emitted from the explosive device $\left(\frac{K_{^{1}\mathrm{H}}(E_{\gamma 1})}{K_{^{14}\mathrm{N}}(E_{\gamma 2})}\right)$ can be written as:

$$\frac{K_{^{1}\mathrm{H}}(E_{\gamma 1})}{K_{^{14}\mathrm{N}}(E_{\gamma 2})} \approx \frac{N_{^{1}\mathrm{H}}}{N_{^{14}\mathrm{N}}} \cdot \left[\frac{\sigma_{^{1}\mathrm{H}}(E_{\mathrm{n}})}{\sigma_{^{14}\mathrm{N}}(E_{\mathrm{n}})}\right]_{\mathrm{T}} \cdot \frac{f_{^{1}\mathrm{H}}(E_{\gamma 1})}{f_{^{14}\mathrm{N}}(E_{\gamma 2})} \cdot \frac{\int_{V} n_{^{14}\mathrm{N}}(\vec{r}) \cdot P(\vec{r}, E_{\gamma 1}) \cdot \mathrm{d}V}{\int_{V} n_{^{14}\mathrm{N}}(\vec{r}) \cdot P(\vec{r}, E_{\gamma 2}) \cdot \mathrm{d}V}, \tag{4}$$

where $E_{\gamma 1}$ and $E_{\gamma 2}$ are the energies of the characteristic γ-rays of ^{1}H and ^{14}N, respectively.

Since the abundances of ^{1}H, ^{12}C, ^{14}N, and ^{16}O are constant in the explosive (they are 99.99, 98.93, 99.63, and 99.76%, respectively), the element number ratios of H, C, N, and O can be deduced according to the ratios of the numbers of ^{1}H, ^{12}C, ^{14}N, and ^{16}O. In this paper, it was assumed that ^{1}H, ^{12}C, ^{14}N, and ^{16}O occupy all of the nuclei of H, C, N, and O, so that the abundances of ^{1}H, ^{12}C, ^{14}N, and ^{16}O were all assumed 100% in the simulation. Therefore, the equation for the element number ratio between H and N of the concealed explosive ([H]/[N]) is given by:

$$[\mathrm{H}]/[\mathrm{N}] = \frac{N_{^{1}\mathrm{H}}}{N_{^{14}\mathrm{N}}} \cdot \frac{A_{^{1}\mathrm{H}}}{A_{^{14}\mathrm{N}}} \approx \frac{\frac{K_{^{1}\mathrm{H}}(E_{\gamma 1})}{K_{^{14}\mathrm{N}}(E_{\gamma 2})} \cdot \frac{A_{^{1}\mathrm{H}}}{A_{^{14}\mathrm{N}}}}{\left[\frac{\sigma_{^{1}\mathrm{H}}(E_{\mathrm{n}})}{\sigma_{^{14}\mathrm{N}}(E_{\mathrm{n}})}\right]_{\mathrm{T}} \cdot \frac{f_{^{1}\mathrm{H}}(E_{\gamma 1})}{f_{^{14}\mathrm{N}}(E_{\gamma 2})} \cdot \frac{\int_{V} n_{^{14}\mathrm{N}}(\vec{r}) \cdot P(\vec{r}, E_{\gamma 1}) \cdot \mathrm{d}V}{\int_{V} n_{^{14}\mathrm{N}}(\vec{r}) \cdot P(\vec{r}, E_{\gamma 2}) \cdot \mathrm{d}V}}, \tag{5}$$

where $A_{^{1}\mathrm{H}}$ and $A_{^{14}\mathrm{N}}$ are the abundances of ^{1}H and ^{14}N, respectively. The equations for [C]/[N] and [O]/[N] can be also obtained in a similar way.

In Eq. (5), $\int_{V} n_{^{14}\mathrm{N}}(\vec{r}) \cdot P(\vec{r}, E_{\gamma}) \cdot \mathrm{d}V$ is the absorption efficiency for the explosive device of γ-rays. Assuming that the radial profiles of the γ emissions from the different nuclei are the same, which is justified by the identical energy dependence of the (n,γ) cross sections for the different nuclei as shown in Fig. 1, the absorption efficiency only depends on the energy of the γ-ray. The absorption

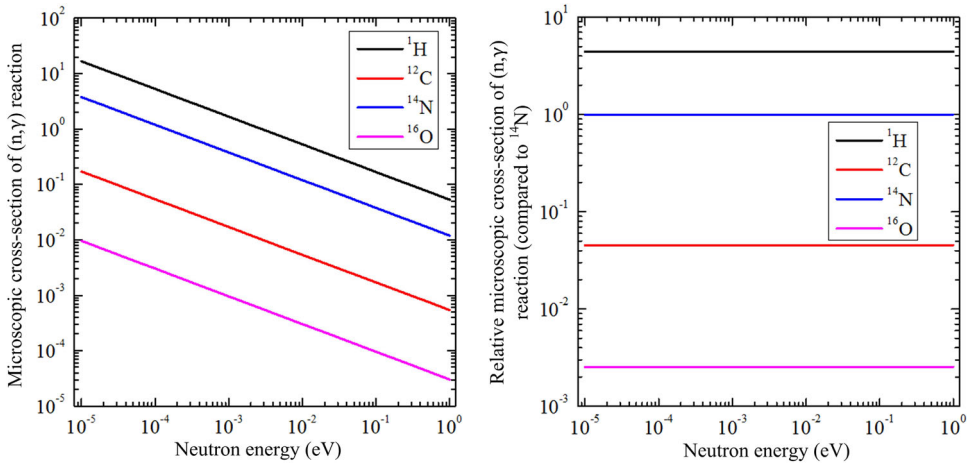

Fig. 1 (Color online) Microscopic cross sections of the (n,γ) reactions of ^{1}H, ^{12}C, ^{14}N, and ^{16}O

efficiency $F(E_\gamma)$ can be expressed by the following equation using Eq. (1):

$$F(E_\gamma) = \int_V n_{^{14}\mathrm{N}}(\vec{r}) \cdot P(\vec{r}, E_\gamma) \cdot \mathrm{d}V = \frac{K_{^{14}\mathrm{N}}(E_\gamma)}{f_{^{14}\mathrm{N}}(E_\gamma)}. \quad (6)$$

Therefore, by measuring the strengths of the various characteristic γ-rays of ^{14}N outgoing from the explosive device and calculating the ratios between the strengths and branch ratios, the absorption efficiencies can be calibrated. Then, the absorption efficiencies for the characteristic γ-rays of other nuclides can be deduced by performing an energy interpolation calculation:

$$F(E_{\gamma 0}) = F(E_{\gamma 1}) + [F(E_{\gamma 1}) - F(E_{\gamma 2})] \cdot \frac{E_{\gamma 0} - E_{\gamma 1}}{E_{\gamma 1} - E_{\gamma 2}}, \quad (7)$$

where $E_{\gamma 0}$ is the energy of the required characteristic γ ray; and $E_{\gamma 1}$ and $E_{\gamma 2}$ are the energies of the characteristic γ-rays of ^{14}N closest to $E_{\gamma 0}$.

3 Numerical simulation study

In order to verify the feasibility of the element analysis method of concealed explosives based on TNA, a numerical simulation study based on a numerical simulation platform was carried out.

The numerical simulation platform consists of three parts: physical models, a transport program based on the JMCT software, and a data processing program. The physical models include a concealed explosive, shield, thermal neutron source, and γ-ray detector, as shown in Fig. 2. The concealed explosive is ball-shaped with a radius of 10 cm and RDX composition (formula $C_3H_6N_6O_6$ and mass of $\sim$ 7.6 kg). The shield is a spherical Al shell surrounding the concealed explosive with a thickness of 1 cm and an outer radius of 15 cm. The thermal neutron source is a point source with an intensity of 10^8 s^{-1}, placed 20 cm away from the center of the concealed explosive, and the thermal neutrons are emitted isotropically with energies 0.025 eV. The γ-ray detector is an HPGe detector with a size Φ65 mm × 60 mm, placed 20 cm away from the center of the concealed explosive.

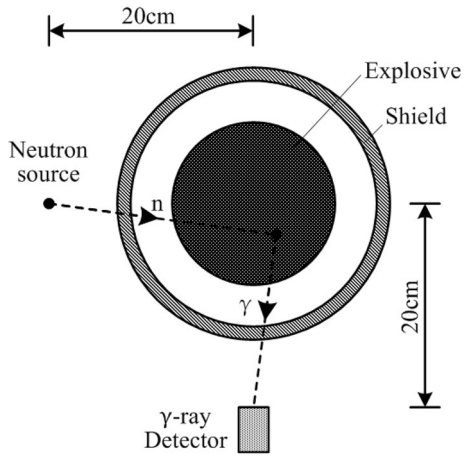

Fig. 2 Physical models in the numerical simulation study

The physical models were imported into the transport program based on JMCT software. The JMCT software is a Monte Carlo particle transport simulation software developed by the Beijing Institute of Applied Physics and Computational Mathematics and Software Center for High Performance Numerical Simulation, China Academy of Engineering Physics. It can precisely simulate neutron, photon, and neutron–photon coupled transport and has the abilities of 3D visualization modeling and high-speed parallel computation [20, 21]. Nowadays, the JMCT software is applied to simulation studies of physical designs of reactors, radiation detection techniques, and arms control verification techniques. In the transport program, the neutron transport in the explosive device (including the concealed explosive and Al shield), and the production and emission of the characteristic γ-rays of the explosive nuclides were simulated with high precision.

Lastly, the data processing program based on C++ was used to analyze the spectrum of the γ-rays emitted from the explosive device, calibrate the absorption efficiencies of the explosive device to γ-rays, and reconstruct the element number ratios of the concealed explosive.

4 Discussion

Using the numerical simulation, the spectrum of the γ-rays emitted from the explosive device (the irradiation time of the thermal neutrons was 1 s) was achieved and is shown in Fig. 3. It is important to note that the detector's response to the γ-rays was not taken into account, and is discussed in the last paragraph of Sect. 4. In Fig. 3, the counts of the γ-rays emitted from the explosive device are calculated by Tally 1 of the JMCT software, which is used to count the numbers of the particles (neutron or photon) passing through the surfaces. The peaks of the characteristic γ-rays of the (n,γ) reactions of ^{1}H, ^{12}C, and ^{14}N are marked in Fig. 3 (the energy bin of each channel is 1 keV), and the peak counts of the characteristic γ-rays of ^{12}C were the lowest. It should be noted that the peak of the characteristic γ-rays of ^{16}O is not observed in Fig. 3. This is because the microscopic cross section of the (n,γ) reaction of ^{16}O is too small and far smaller than those of ^{1}H, ^{12}C, and ^{14}N. Therefore, there were a few characteristic γ-rays of the ^{16}O(n,γ) reactions emitted from the explosive device, and they were swallowed by the background. As a result, the detection of ^{16}O will not be discussed further in this

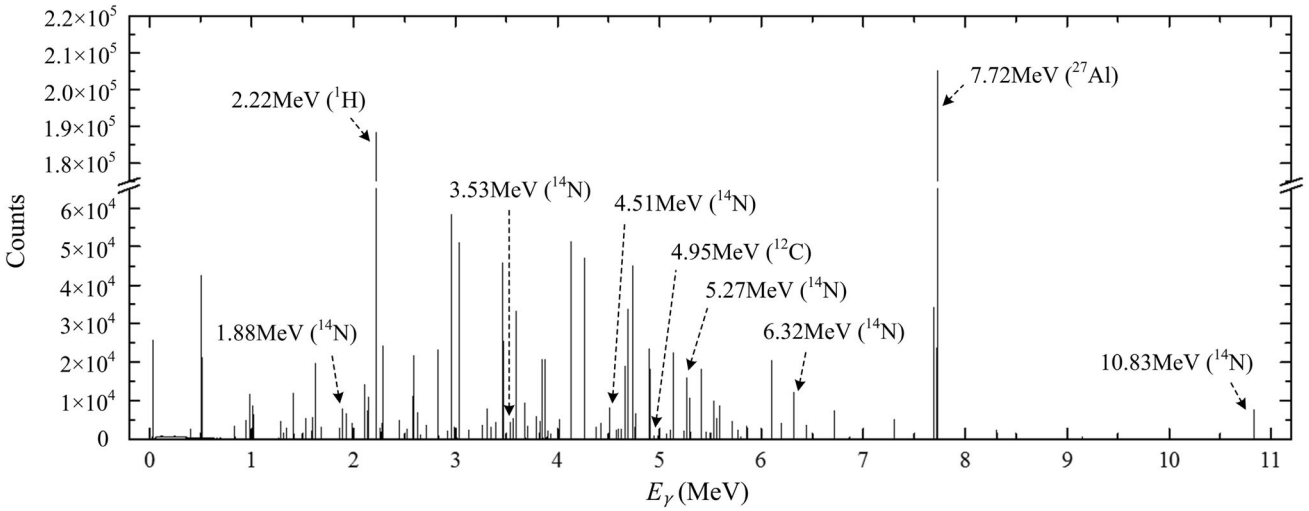

Fig. 3 Energy spectrum of γ-rays emitted from the explosive device

paper, and we will focus on the detection of ^{1}H, ^{12}C, and ^{14}N, including the calculation of the element number ratios, such as [H]/[N] and [C]/[N].

By counting the peak counts of the series of characteristic γ-rays of ^{14}N emitted from the explosive device (see Table 1) and calculating the ratios between the peak counts and branching ratios of the characteristic γ-rays, the absorption efficiencies of the explosive device to γ-rays can be calibrated, as shown in Fig. 4. The data in Fig. 4 are normalized to 10.83 MeV γ-rays. It is noted that in counting the peak counts of the characteristic γ-rays of the explosive nuclides, the interference of the background should be removed to obtain accurate counts.

By counting the peak counts of the characteristic γ-rays of ^{1}H, ^{12}C, and ^{14}N (see Table 1) emitted from the explosive device, and combining the equations in Sect. 2, the element number ratios of the concealed explosive, including [H]/[N] and [C]/[N], can be calculated and are given in Table 2. In Table 2 the errors of the reconstructed values of [H]/[N] and [C]/[N] are less than 5%. Therefore, the element analysis method of concealed explosives based on TNA had a high reconstruction precision for the element number ratios of the concealed explosive. It should be noted that if the absorption efficiencies of the explosive device to γ-rays are not calibrated (namely the absorption efficiencies all equals 1), the errors of the reconstructed [H]/[N] and [C]/[N] would deteriorate to 25.8 and 7.0%, respectively. Besides, compared with the reconstructed accuracy of [H]/[N] of the explosives in Ref. [15] (the errors range from 5 to 23%), where the absorption efficiencies from the numerical simulation are used with the experimental data, the reconstruction accuracy in this paper is clearly higher.

Furthermore, the element number ratios of some typical materials (including explosives, drugs, and common materials) in the shielding environment were reconstructed on the numerical simulation platform, and the details are provided in Table 3 [22]. The shield is the same as for the shield model in Sect. 3, and the shapes and volumes of the concealed materials are the same as those of the explosive model in Sect. 3. The reconstructed element number ratios of these materials are plotted in a scatter diagram in Fig. 5. In Table 3 and Fig. 5, the element number ratios of the

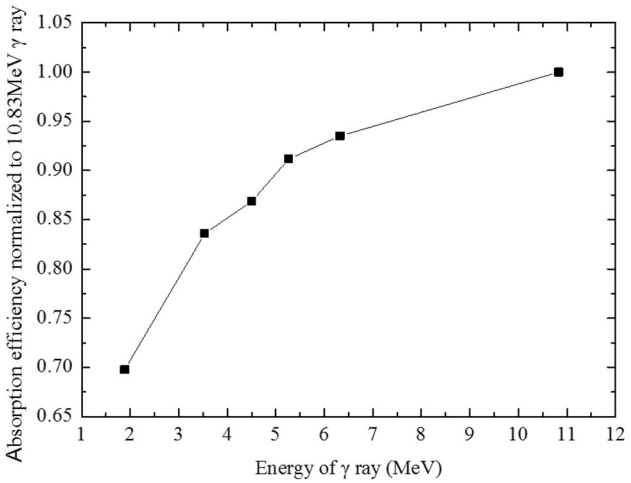

Fig. 4 Absorption efficiency of the explosive device to γ rays

Table 2 Reconstruction results of the element number ratios of the concealed explosive

Element number ratio	Actual value	Reconstruction result
[H]/[N]	1	1.02
[C]/[N]	0.5	0.521

Table 3 Reconstruction results of the element number ratios of various materials

	Material	Molecular formula	[H]/[N]		[C]/[N]	
			Actual value	Reconstruction	Actual value	Reconstruction
Explosive	RDX	$C_3H_6N_6O_6$	1	1.02	0.5	0.521
	TNT	$C_7H_5N_3O_6$	1.67	1.67	2.33	2.46
	Nitroglycerin	$C_3H_5N_3O_9$	1.67	1.69	1	1.01
	Ammonium nitrate	NH_4NO_3	2	1.99	0	0.00
Drug	Morphine	$C_{17}H_{19}NO_3$	19	19.0	17	17.4
	Cocaine	$C_{17}H_{21}NO_4$	21	20.8	17	17.2
	Heroin	$C_{21}H_{23}NO_5$	23	22.7	21	21.3
Common material	Polyurethane	$CHNO_2$	1	1.01	1	1.02
	Nylon-6	$C_6H_{13}NO$	13	12.7	6	6.43
	Urea	CH_4N_2O	2	2.02	0.5	0.504

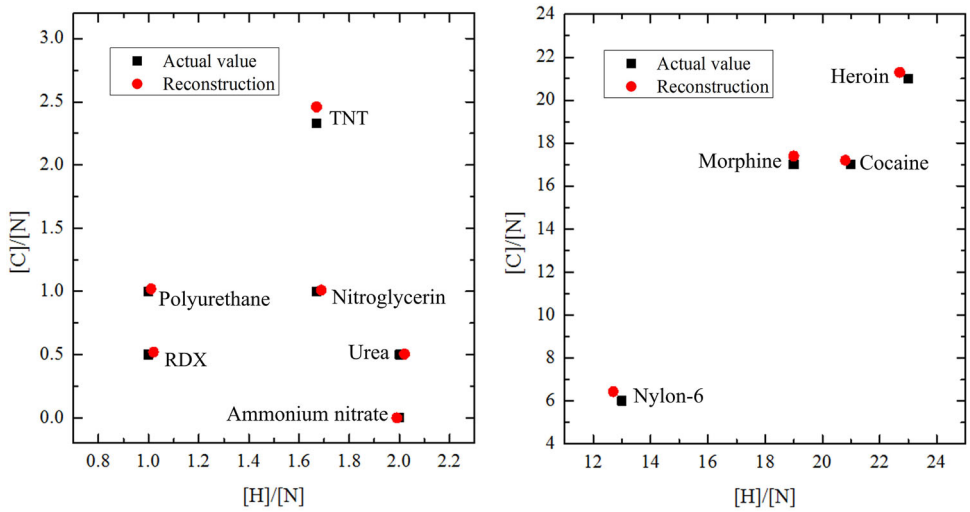

Fig. 5 (Color online) Reconstruction results of the element number ratios of various materials (scatter diagram)

materials are different and the reconstruction results of the element number ratios are accurate; therefore, these materials were easily distinguished based on the reconstructed element number ratios (including [H]/[N] and [C]/[N]). Generally, due to the particularity of the chemical structures of explosives, the element number ratios of explosives are mainly different from those of common materials. Therefore, explosives can be effectively discriminated from common materials by comparing their element number ratios. Besides, the element number ratios of different explosives are always varied and can be used to represent the explosive types. As a result, although the element analysis method of concealed explosives based on TNA cannot discriminate materials with the same [H]/[N] and [C]/[N], it can be still be applied to determine the existence of explosives and identify explosive types due to its high reconstruction accuracy of the element number ratios of concealed materials.

However, the γ detector used in the element analysis method of concealed explosives based on TNA should have two qualifications: a high energy resolution and proper detection efficiency. For example, by considering the model parameters in Sect. 3 (including the thermal neutron source, concealed explosive, and shield), in order to discriminate the full-energy peaks of the characteristic γ-rays of ^{1}H, ^{12}C, and ^{14}N, the energy resolution (FWHM) of the γ detector should be greater than 1%; meanwhile, in order to achieve the detection of the characteristic γ-rays of ^{12}C in 1 h (the count uncertainty of the full-energy peak is less than 5%), the detection efficiency (absolute efficiency) of the γ detector to the full-energy peak of the characteristic γ-rays with energies of 4.95 MeV emitted from the explosive device should be greater than 1.4×10^{-4}. After the calculation of the model parameters in Sect. 3, an HPGe detector (ORTEC company) with size Φ65 mm × 60 mm and placed 20 cm away from the center of the concealed explosive (with a 90° angle between the neutron

source and γ detector relative to the center of the concealed explosive, as shown in Fig. 2) fulfilled the two qualifications above.

5 Conclusion

In this paper, an element analysis method of concealed explosives based on TNA was proposed. This method can be used to determine the existence of concealed bulk explosives and identify explosive types. First, this paper introduced the principles of this method and established a mathematical model that allows for the calculation of the element number ratio of the concealed explosive. Second, a numerical simulation platform of this method was established on the basis of the JMCT software and was used to simulate the neutron transport in the explosive device model (including the explosive and shield models) and the production and emission of the characteristic γ-rays of the explosive nuclides. Then, the element number ratios of the explosive model were reconstructed through the calibration of the absorption efficiencies of the explosive device to γ rays, and the reconstruction results were in good agreement with the actual values demonstrating the high reconstruction precision of this method. Lastly, through the simulation study, the method was used to discriminate explosives, drugs, and common materials, demonstrating that it has the abilities to determine the existence of concealed bulk explosives and identifying explosive types, suitable for use in airport security and customs inspections. It should be noted that the main focus of this paper was on the detection of concealed explosives of several kilograms. For the concealed explosives of only several hundred grams, the element analysis method of concealed explosives based on TNA is also suitable and is able to reconstruct the element number ratios of the explosives accurately, but the measurement time to achieve the equivalent counts of the characteristic γ-rays of explosive nuclides will increase.

References

1. K. Huang, Y.B. Lin, T.F. Wu et al., The overview of the foreign technologies of explosives detection and identification. Explos. Mater. **36**, 34–38 (2007). **(In Chinese)**
2. P. Gao, Y.H. Jin, G.J. Zhang et al., Design of explosive detection system based on NQR theory. Eng. Equip. Res. **27**(1), 5–9 (2008). **(In Chinese)**
3. M. Ostafin, B. Nogaj, ^{14}N-NQR based device for detection of explosives in landmines. Measurement **40**, 43–54 (2007). https://doi.org/10.1016/j.measurement.2006.04.003
4. H. Liu, J.M. Shi, L. Cheng et al., Stand-off detection technology of explosives. Laser Infrared **45**, 733–739 (2015). **(In Chinese)**
5. Z.D. Whetstone, K.J. Kearfott, A review of conventional explosives detection using active neutron interrogation. J. Radioanal. Nucl. Chem. **301**, 629–639 (2014). https://doi.org/10.1007/s10967-014-3260-5
6. W. Ding, Y. Dou, G. Wang et al., Review on detection technology for explosives. Explos. Mater. **40**, 33–37 (2011). **(In Chinese)**
7. S.K. Sharma, S. Jakhar, R. Shukla et al., Explosive detection system using pulsed 14 MeV neutron source. Fusion Eng. Des. **85**, 1562–1564 (2010). https://doi.org/10.1016/j.fusengdes.2010.04.044
8. G. Vourvopoulos, F.J. Schultz, A pulsed fast-thermal neutron system for the detection of hidden explosives. Nucl. Instrum. Methods B **79**, 585–588 (1993). https://doi.org/10.1016/0168-583X(93)95419-6
9. E.L. Reber, L.G. Blackwood, A.J. Edwards, Idaho explosives detection system. Nucl. Instrum. Methods B **241**, 738–742 (2005). https://doi.org/10.1016/j.nimb.2005.07.235
10. Y. Xiang, Z. Xiong, G. Hu et al., Detecting dynamite by active method. Nucl. Tech. **28**, 872–876 (2005). **(In Chinese)**
11. P. Shea, T. Gozani, H. Bozorgmanesh, A TNA explosives-detection system in airline baggage. Nucl. Instrum. Methods A **299**, 444–448 (1990). https://doi.org/10.1016/0168-9002(90)90822-N
12. J.E. McFee, T. Cousins, T. Jones et al., A thermal neutron activation system for confirmatory nonmetallic land mine detection, in *SPIE Conference on Detection and Remediation Technologies for Mines and Minelike Targets III. Proc SPIE*, vol 3392, pp. 553–564 (1998)
13. E. Clifford, H. Ing, J. McFee et al., High rate counting electronics for a thermal neutron analysis land mine detector, in *SPIE Conference on Penetrating Radiation Systems and Applications. Proc SPIE*, vol 3769, pp. 155–166 (1999). https://doi.org/10.1117/12.363677
14. E. Clifford, J. McFee, H. Ing et al., A militarily fielded thermal neutron activation sensor for landmine detection. Nucl. Instrum. Methods A **579**, 418–425 (2007). https://doi.org/10.1016/j.nima.2007.04.091
15. Y. Xiang, G. Hu, J. Zhang, On the method of actively detecting composition of dynamite. China Nucl. Sci. Technol. Rep. **1**, 84–94 (2005). **(In Chinese)**
16. W.V. Nunes, A.X. da Silva, V.R. Crispim et al., Explosives detection using prompt-gamma neutron activation and neural networks. Appl. Radiat. Isot. **56**, 937–943 (2002). https://doi.org/10.1016/S0969-8043(02)00059-3
17. T.J. Shaw, D. Brown, J. D'Arcy et al., Small threat and contraband detection with TNA-based systems. Appl. Radiat. Isot. **63**, 779–782 (2005). https://doi.org/10.1016/j.apradiso.2005.05.036
18. H. Wang, Y. Li, Y. Yang et al., Study of explosive detection with PFTNA method and neural network. Nucl. Electron. Detect. Technol. **25**, 384–387 (2005). **(In Chinese)**
19. ENDF: Evaluated Nuclear Data File [EB/OL], 09 Nov 2016. https://www-nds.iaea.org/exfor/endf.htm
20. G. Li, B. Zhang, L. Deng et al., Development of Monte Carlo particle transport code JMCT. High Power Laser Part. Beams **25**, 158–162 (2013). **(In Chinese)**
21. L. Deng, G. Li, B. Zhang et al., Simulation of Full-core pin-by-pin Model by JMCT Monte Carlo Neutron-photon Transport Code. At. Energy Sci. Technol. **48**, 1061–1066 (2014). **(In Chinese)**
22. S. Xu, W. Zhu, An explosive and drug detection method based on associated particle imaging. At. Energy Sci. Technol. **32**, 482–486 (1998). **(In Chinese)**